Two-Photon Imaging of Cortical Microcirculation

David Kleinfeld[1] and Winfried Denk[2]

1- Department of Physics, University of California, La Jolla, CA 92093.

2- Max-Planck Institute for Medical Research Department of Biomedical Optics Jahn-Str. 29, D-69120 Heidelberg, Germany.

Goal. Brain homeostasis depends on adequate levels of blood flow to insure the delivery of nutrients and to facilitate the removal of catabolic products. The exchange of material between constituents in the blood and neurons and glia occurs at the level of individual capillaries, vessels that are 5 to 8 μm in caliber. An increase in the electrical activity within populations of neurons may result in transient increases and decreases of blood flow in activated and nearby quiescent regions, respectively (Woolsey et al., 1996). Here we describe how cortical blood flow at the level of individual capillaries can be observed with high resolution imaging techniques (Dirnagl et al., 1992; Kleinfeld and Denk, 2000; Kleinfeld et al., 1998; Villringer et al., 1989).

Area of Application. These redistributions of blood flow, together with changes in the blood oxygenation levels, form the basis of functional MRI (Ogawa et al., 1990) and intrinsic optical imaging (Blasdel and Salama, 1986; Grinvald et al., 1986). The study of capillary flow in parallel with measures of cell physiology forms the basis of understanding this imaging modality. A second area is the study of blood flow in conjunction with the study of stroke models (Pinard et al., 2002; Schaffer et al., 2003).

Materials. The most common species used in previous studies have been Wistar or Sprague-Dawley rats and Swiss-Webster mice (Hudetz, 1997; Woolsey et al., 1996). Whole animal imaging experiments usually require the use of an anesthetic to immobilize the animal in a calm and pain free state (Flecknell, 1987; Short, 1987);

although the use of awake but immobilized preparations (Kleinfeld et al., 2002; Ono et al., 1986) or awake animals with a fiber microscope (Helmchen et al., 2001) is an alternate possibility Anesthetics by their nature have a strong effect on the activity in the nervous system and therefore on the hemodynamics that is coupled to neural activity (Table I). Beyond these issues, the microscopy follows standard 2PLSM (Denk et al., 1990; Tsai et al., 2002) in conjunction with whole animal (Denk et al., 1994; Kleinfeld et al., 1998; Lendvai et al., 2000; Svoboda et al., 1997) techniques.

Protocol and procedures. Pharmaceuticals and surgical supplies were obtained from Henry Schein (Melville, NY). Animals were anesthetized with urethane at an initial level of 1.2 g/kg, delivered i.p. as a split dose over a period of 10 minutes, and were supplemented at 0.2 g/kg as needed. Animals received a prophylactic dose of atropine (0.1 mg s.c. every 2 h) as a prelude against respiratory distress. Body fluids were supplemented through an s.c. injection of physiological saline (0.9 % (w/v) NaCl) supplemented with 5 % (w/v) dextrose (10 ml/kg/hr). The eyes were protected against desiccation by drops of mineral oil. Body temperature was maintained near 37.0°C using a heating blanket (no. 507053, Harvard Instruments, Holliston, MA).

The animal was secured in a stereotaxic holder (no. 960, David Kopf Instruments, Tujunga, CA) modified to rotate about the A-P axis. A succession of glancing cuts along an outline of the desired craniotomy were made with a high speed handpiece (Midwest no. 464004, Patterson Dental Supply, Saint Paul, MN) equipped with a 1/2 round bur. We ceased to cut just as the bone was observed to craze. The resulting bone flap was removed with forceps, and the now exposed surface of the dura was protected from desiccation with a gelatin sponge (NDC 0009-0364-01, Upjohn, Kalamazoo, MI) soaked with physiological saline.

A metal frame was fixed to the skull that surrounds the craniotomy as a means to rigidly hold the head of the animal to the optical apparatus (Kleinfeld and Delaney, 1996). The frame was directly glued to the skull with dental acrylic cement. To achieve a reliable connection between acrylic and bone, the contact regions on the bone were first carefully cleaned of soft tissue and rubbed with a cotton applicator, then a thin layer of

cyanoacrylate cement (Superbonder 49550; Loctite, Hartford, CT) was applied, finally the skull was rubbed again to remove excess cyanoacrylate. The dura was removed after the frame was attached to the rat. The chamber was sealed using a cover glass (no. 1, cut to size) after filling the interior of the chamber with 1 to 2 % (w/v) low melting point agarose (no. A-9793, Sigma, St. Louis, MO) dissolved in artificial cerebral spinal fluid (ASCF, composition in mM: NaCl 125, KCl 5, Glucose 10 , HEPES 10, $CaCl_2$ 3.1, $MgCl_2$ 1.3; pH 7.4) that contained neither carbonate nor phosphate which cause precipitation when the solution is boiled to dissolve the agarose.

Blood plasma is labeled through a tail-vein injection. The tail is submerged in 37°C water for approximately 2 minutes to make the veins dilate and then a soft clamp is placed at the base of the tail. Starting as close to the tip of the tail as possible, a 24 gauge catheter is inserted and, for 250 g rats, a 0.5 ml bolus of 5 % (w/v) solution of fluorescein isothiocynate (FITC) dextran (70 kD; FD-70, Sigma, St. Louis, MO) is injected to label the blood serum

Short example of application. The angioarchitecture of a cube of cortex, approximately 100 μm on edge and containing microvessels, was imaged (Fig. 1a). Successive, rapidly acquired planar images of such microvessels revealed a succession of dark objects that moved across a sea of fluorescently labeled serum (Fig. 1b). The dark spots are red blood cells (RBCs), which exclude the dye and are therefore not fluorescent (Dirnagl et al., 1992). The change in position of the spots between successive images is proportional to the velocity (arrows; Fig. 1b). To achieve high time resolution, we acquired repetitive scans along the central axis of a capillary to characterize the flow of RBCs in capillaries. The motion of RBCs leads to dark bands in the data set (Fig. 1c). The average time between bands at a fixed position, denoted Δt, is inversely proportional to the flux, the average distance between bands at a fixed time, denoted Δx, is inversely proportional to the density of RBCs, and the average slope of the band, $\Delta t/\Delta x$, is inversely proportional to the velocity of the RBCs (Fig. 1c). These three quantities are related by **flux = density • velocity**. A particularly interesting case involves flow at a “T”-junction, for which 2 of the 3 arms may be simultaneously imaged. For the examples of figures 1d and 1e, the flow is seen to spontaneously reverse

direction in one of the arms.

Advantages and Limits. Two photon laser scanning microscopy can be used to image the flow of red blood cells at least 600 μm below the pial surface in rat. This range encompasses layer 2/3 of neocortex as well as the superficial part of layer 4, the level of the dominant thalamic input to neocortex. It is likely that future studies will be of greatest value when blood flow measurements are performed simultaneously with measurements of neighboring neuronal or glial activity.

Table 1 - Anesthetics and doses used in studies of cerebral blood flow in rat

Agent (delivered i.p.)	**Initial Dose** (per kg rat)	**Supplement** (per kg rat)	**Representative reference**
a-chloralose	50 mg	40 mg/hr	(Lindauer et al., 1993)
Ketamine plus Xylazine	100 mg 50 mg	30 mg 15 mg as required	(Wei et al., 1995)
Sodium pentabarbatol	60 mg	10 mg as required	(Rovainen et al., 1993)
Sodium pentabarbatol plus Ketamine	25 mg 30 mg		(Hudetz et al., 1992)
Urethane	1000 mg	100 mg as required	(Kleinfeld et al., 1998)
Urethane plus a-chloralose	600 mg 50 mg		(Ngai et al., 1988)

Dosing is approximate and will change depending on the emotional state of the animal.

References

Blasdel, G. G., and Salama, G. (1986). Voltage-sensitive dyes reveal a modular organization in monkey striate cortex. Nature *321*, 579-585.

Denk, W., Delaney, K. R., Kleinfeld, D., Strowbridge, B., Tank, D. W., and Yuste, R. (1994). Anatomical and functional imaging of neurons and circuits using two photon laser scanning microscopy. Journal of Neuroscience Methods *54*, 151-162.

Denk, W., Strickler, J. H., and Webb, W. W. (1990). Two-photon laser scanning fluorescence microscopy. Science *248*, 73-76.

Dirnagl, U., Villringer, A., and Einhaupl, K. M. (1992). *In-vivo* confocal scanning laser microscopy of the cerebral microcirculation. Journal of Microscopy *165*, 147-157.

Flecknell, P. A. (1987). Laboratory Animal Anesthesia: An Introduction for Research Workers and Technicians (San Diego, Academic Press).

Grinvald, A., Lieke, E. E., Frostig, R. D., Gilbert, C. D., and Wiesel, T. N. (1986). Functional architecture of cortex revealed by optical imaging of intrinsic signals. Nature *324*, 361-364.

Helmchen, F., Fee, M. S., Tank, D. W., and Denk , W. (2001). A miniature head-mounted two-photon microscope: High-resolution brain imaging in freely moving animals. Neuron *31*, 903-912.

Hudetz, A. G. (1997). Blood Flow in the cerebral capillary network: A review emphasizing observations with intravital microscopy. Microcirculation *4*, 233-252.

Hudetz, A. G., Weigle, C. G. M., Fendy, F. J., and Roman, R. J. (1992). Use of fluorescently labeled erythrocytes and digital cross-correlation for the measurement of flow velocity in the cerebral microcirculation. Microvascular Research *43*, 334-341.

Kleinfeld, D., and Delaney, K. R. (1996). Distributed representation of vibrissa movement in the upper layers of somatosensory cortex revealed with voltage sensitive dyes. Journal of Comparative Neurology *375*, 89-108.

Kleinfeld, D., and Denk, W. (2000). Two-photon imaging of neocortical microcirculation. In Imaging Neurons: A Laboratory Manual, R. Yuste, F. Lanni, and A. Konnerth, eds. (Cold Spring Harbor, Cold Spring Harbor Laboratory Press), pp. 23.21-23.15.

Kleinfeld, D., Mitra, P. P., Helmchen, F., and Denk, W. (1998). Fluctuations and stimulus-induced changes in blood flow observed in individual capillaries in layers 2 through 4 of rat neocortex. Proceedings of the National Academy of Sciences USA *95*, 15741-15746.

Kleinfeld, D., Sachdev, R. N. S., Merchant, L. M., Jarvis, M. R., and Ebner, F. F. (2002). Adaptive filtering of vibrissa input in motor cortex of rat. Neuron *34*, 1021-1034.

Lendvai, B., Stern, E. A., Chen, B., and Svoboda, K. (2000). Experience-dependent plasticity of dendritic spines in the developing rat barrel cortex in vivo. Nature *404*, 876-881.

Lindauer, U., Villringer, A., and Dirnagl, U. (1993). Characterization of CBF response to somatosensory stimulation: Model and influence of anesthetics. American Journal of Physiology *264*, H1223-H1228.

Ngai, A. C., Ko, K. R., Morii, S., and Winn, H. R. (1988). Effect of sciatic nerve stimulation on pial arterioles in rats. American Journal of Physiology *254*, H133-H139.

Ogawa, S., Lee, T.-m., Nayak, A. S., and Glynn, P. (1990). Oxygenation-sensitive contrast in magnetic resonance image of rodent brain at high fields. Magnetic Resonance in Medicine *14*, 68-78.

Ono, T., Nakamura, K., Nishijo, H., and Fukuda, M. (1986). Hypothalamic neuron involvement in integration of reward, aversion and cue signals. Journal of Neurophysiology *56*, 63-79.

Pinard, E., Nallet, MacKenzie, E. T., Seylaz, J., and Roussel, S. (2002). Penumbral microcirculatory changes associated with peri-infarct depolarizations in the rat. Stroke *33*, 606-612.

Rovainen, C. M., Woolsey, T. A., Blocher, N. C., Wang, D.-B., and Robinson, O. F. (1993). Blood flow in single surface arterioles and venules on the mouse somatosensory cortex measured with videomicroscopy, fluorescent dextrans, nonoccluding fluorescent beads, and computer-assisted image analysis. Journal of Cerebral Blood Flow and Metabolism *13*, 359-371.

Schaffer, C. B., Tsai, P. S., Nishimura, N., Schroeder, L. F., Friedman, B., Lyden, P. D., Ebner, F. F., and Kleinfeld, D. (2003). All optical thrombotic stroke model for near-surface blood vessels in rat: Focal illumination of exogenous photosensitizers combined with real-time two-photon imaging. Paper presented at: SPIE Photonics West (San Jose).

Short, C. E. (1987). Principles and Practice of Veterinary Anesthesia (Baltimore, Williams and Willisms).

Svoboda, K., Denk, W., Kleinfeld, D., and Tank, D. W. (1997). In vivo dendritic calcium dynamics in neocortical pyramidal neurons. Nature *385*, 161-165.

Tsai, P. S., Nishimura, N., Yoder, E. J., Dolnick, E. M., White, G. A., and Kleinfeld, D. (2002). Principles, design, and construction of a two photon laser scanning microscope for in vitro and in vivo brain imaging. In In Vivo Optical Imaging of Brain Function, R. D. Frostig, ed. (Broca Raton, CRC Press), pp. 113-171.

Villringer, A., Haberl, R. L., Dirnagl, U., Anneser, F., Verst, M., and Einhaupl, K. M. (1989). Confocal laser microscopy to study microcirculation on the rat brain surface in vivo. Brain Reserach *504*, 159-160.

Wei, L., Rovainen, C. M., and Woolsey, T. A. (1995). Ministrokes in rat barrel cortex. Stroke *26*, 1459-1462.

Woolsey, T. A., Rovainen, C. M., Cox, S. B., Henger, M. H., Liange, G. E., Liu, D., Moskalenko, Y. E., Sui, J., and Wei, L. (1996). Neuronal units linked to microvascular modules in cerebral cortex: Response elements for imaging the brain. Cerebral Cortex *6*, 647-660.

Figure Legend

Figure 1. Parameterization of blood flow in a capillary.

(a) Horizontal view in the vicinity of a capillary. The image is the maximal projection from a contiguous set of 100 planar scans acquired every 1 μm between 310 and 410 μm.

(b) Successive planar images, acquired every 16 ms, through a capillary at a depth of 450 mm. The change in position of a particular unstained object, interpreted as a RBC, is indicated by the series of arrows ( ); the speed of the RBC is 0.11 mm/s.

(c) Line scan through a capillary at a depth of 600 μm. In this imaging modality, the RBCs appear as dark bands. The annotations illustrates how RBC flow can be parameterized as a function of space and time. The instantaneous flux is $1/\Delta t$, the linear density is $1/\Delta x$, and the velocity is $\Delta x/\Delta t$, as indicated.

(d and e) Examples of reversals in the direction of flow observed by simultaneously monitoring RBC motion in two collinear arms of a T-junction at a depth of 260 μm. The lower panel in part d is a planar scan of the junction. The two data sets correspond to approximately 2 s intervals of line-scan measurements that were performed 5 minutes apart. Note the reversals in flow, labeled **R**.

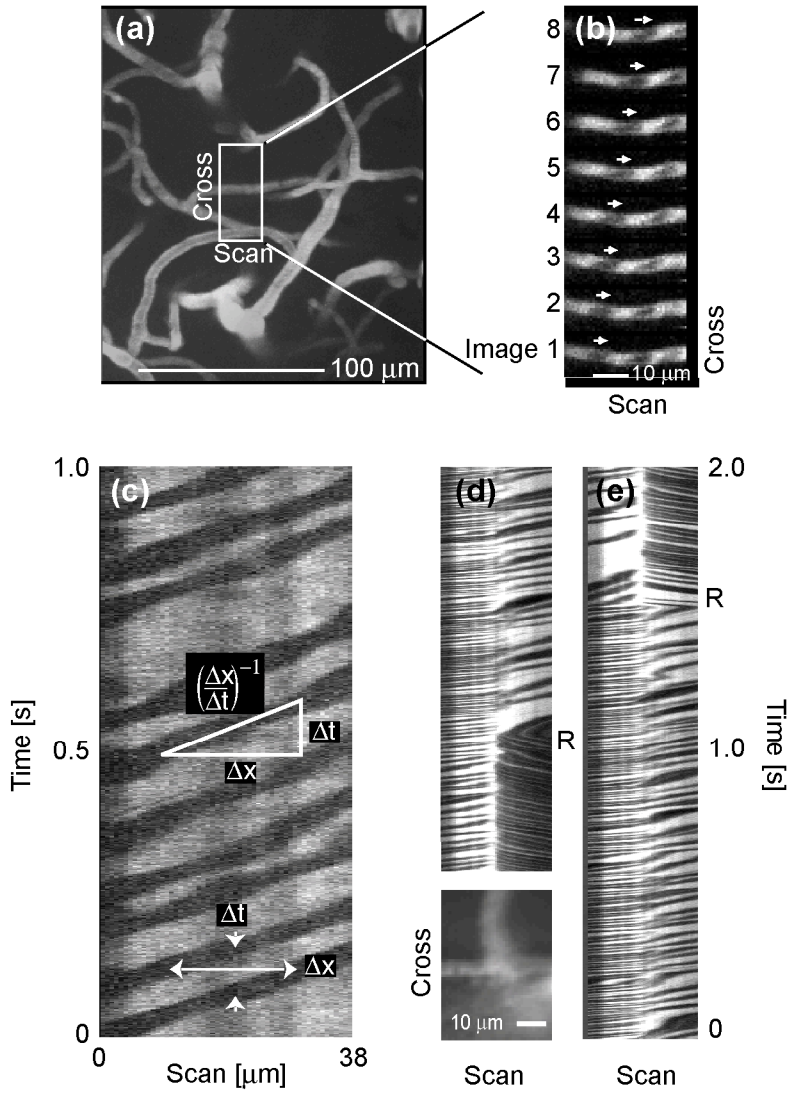

Figure 1 - Kleinfeld and Denk